

Cite this: DOI: 10.1039/c0cc04983b

www.rsc.org/chemcomm

## Rapidly disassembling nanomicelles with disulfide-linked PEG shells for glutathione-mediated intracellular drug delivery†

Hui-Yun Wen,<sup>a</sup> Hai-Qing Dong,<sup>a</sup> Wen-juan Xie,<sup>a</sup> Yong-Yong Li,<sup>\*a</sup> Kang Wang,<sup>a</sup> Giovanni M. Pauletti<sup>c</sup> and Dong-Lu Shi<sup>\*ab</sup>

Received 16th November 2010, Accepted 27th January 2011

DOI: 10.1039/c0cc04983b

**The synthesis and biological efficacy of novel nanomicelles that rapidly disassemble and release their encapsulated payload intracellularly under tumor-relevant glutathione (GSH) levels are reported. The unique design includes a PEG-sheddable shell and poly( $\epsilon$ -benzyloxycarbonyl-L-lysine) core with a redox-sensitive disulfide linkage.**

Surface functionalization with poly(ethylene glycol) (PEG) is one of the leading strategies to prolong the *in vivo* circulation time of nanocarriers in the cardiovascular system due to reduced macrophage clearance.<sup>1</sup> Specifically in cancer therapy, an increased circulation half-life of colloidal drug delivery systems augments accumulation at the tumor site through the enhanced permeability and retention (EPR) effect.<sup>2</sup> However, the hydrophilic shielding layer of PEG that effectively reduces protein opsonization and macrophage uptake may negatively impact cellular uptake and intracellular distribution at the target site due to steric hindrance.<sup>3</sup> Furthermore, the PEG layer may also pose a significant diffusion barrier that negatively affects the release of the encapsulated payload and, consequently, therapeutic efficacy.<sup>4</sup> For example, limited cellular uptake of clinically approved Doxil<sup>®</sup>, which comprises the anticancer agent doxorubicin (DOX) encapsulated within PEG-shielded liposomes<sup>5</sup> contributes to drug resistance of the tumor cells.

Several chemical approaches have been proposed to overcome inadequate pharmacological activity of drugs encapsulated within PEG-shielded nanocarriers. In general, the main objective of these strategies is to remove the PEG shell upon arrival at the target site (*i.e.*, shedding).<sup>6</sup> Szoka and co-workers introduced a sheddable coating design for liposomes using a PEG-diorthoester lipid conjugate.<sup>7</sup> During blood circulation, the orthoester linkage remains fairly stable, limiting bilayer contact and interaction with serum proteins due to PEG-induced steric

hindrance. Under more acidic conditions however, the PEG-lipid conjugate rapidly hydrolyzes leading to bilayer aggregation that accelerates drug release from lipid vesicles.

Successful PEG shedding in response to a biologically relevant stimulus is now recognized as an effective approach to improve therapeutic efficacy of drugs encapsulated in pharmaceutically acceptable nanocarriers.<sup>8</sup> In addition to acid-labile linkers that facilitate drug release following endocytosis into acidic subcellular compartments such as early endosomes, newer strategies attempt to explore redox-sensitive shedding mechanisms.<sup>9</sup> Recently, Kataoka and co-workers reported a 3-fold increase in gene transfection efficiency using PEG-based polyaspartamide micelles as nonviral gene delivery vectors.<sup>10</sup> The authors experimentally demonstrated that gene expression was significantly accelerated in a reducing environment of 10 mM dithiothreitol (DTT). Similarly, release of DOX from reduction-responsive micelles composed of disulfide-linked dextran-*b*-poly( $\epsilon$ -caprolactone) diblock copolymer was much greater in the presence of 10 mM DTT than under non-reducing conditions.<sup>11</sup> Direct experimental evidence of PEG shedding *via* disulfide cleavage in the presence of DTT was recently provided by Langer and co-workers using a novel disulfide-based fluorescence resonance energy transfer (FRET) probe.<sup>12</sup> These data underline the positive impact redox-sensitive PEG shedding may achieve in enhancing therapeutic efficacy of nanosized drug delivery systems in modern medicine. In contrast to DTT, which is an unusually strong reducing agent,<sup>13</sup> cellular redox status *in vivo* is regulated by glutathione (GSH).<sup>14</sup> This ubiquitous molecule is produced intracellularly, maintaining mM concentrations in the cytosol and subcellular compartments. In plasma, however, GSH concentrations are at lower levels ( $\mu$ M) due to rapid enzymatic degradation. Today, GSH is not only recognized as the antioxidant of the cell but also as a key biochemical player in the pathophysiology of human diseases, including cancer.<sup>15</sup>

In this study, we introduce a new nanomicelle design composed of a PEG shell and a poly( $\epsilon$ -benzyloxycarbonyl-L-lysine) core with potential biocompatibility *via* a disulfide linkage (mPEG-SS-PzLL). This unique structure meets the desired therapeutic requirements of high stability during circulation and rapid payload release inside target cells. In the presence of tumor-relevant GSH concentrations, mPEG-SS-PzLL micelles undergo shedding of the PEG shell *via*

<sup>a</sup>The Institute for Advanced Materials and Nano Biomedicine, Tongji University, Shanghai 200092, China. E-mail: yongyong\_li@tongji.edu.cn

<sup>b</sup>Department of Chemical and Materials Engineering, University of Cincinnati, Cincinnati, OH 45221, USA. E-mail: shid@ucmail.uc.edu

<sup>c</sup>James L. Winkle College of Pharmacy, University of Cincinnati, Cincinnati, OH 45267, USA

† Electronic supplementary information (ESI) available: Full experimental method and other data. See DOI: 10.1039/c0cc04983b

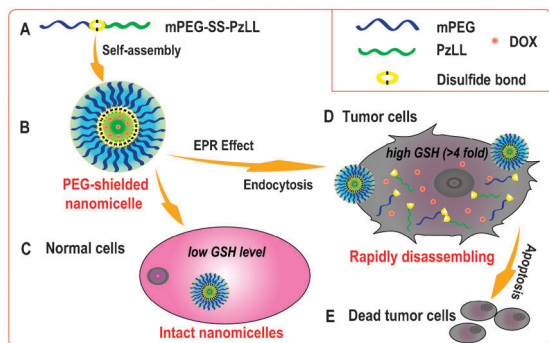


**Fig. 1** Predicted antitumor activity of redox-sensitive DOX-loaded mPEG-SS-PzLL nanomicelles. (A) Amphiphilic block copolymer with disulfide linkage; (B) PEG-shielded nanomicelle; (C) small amount of nanomicelle endocytosis into normal cells (low GSH) resulting in slow drug release; (D) endocytosis of nanomicelles into tumor cells with EPR effect (GSH > 4 fold than normal cells)<sup>9</sup> resulting in rapid drug release; (E) apoptosis of tumor cells.

cleavage of disulfide bonds, followed by rapid disassembly of the original micelle structure facilitating efficient release of the encapsulated payload (Fig. 1).

Briefly, the mPEG-SS-PzLL block copolymers were synthesized by a ring-opening mechanism using amino-terminated modified PEG ( $M_n = 5000$ ) as an initiator (Fig. S1 in ESI<sup>†</sup>). Three different block polymers were prepared by varying the feed ratio of mPEG-SS-NH<sub>2</sub> and zLL-NCA from 1 : 1 to 2 : 3. FTIR spectra showed the stretching vibration of N–H at 3287 cm<sup>-1</sup> and a strong absorbance band at 1731 cm<sup>-1</sup> associated with C=O stretching vibration, which indicated the successful synthesis of the desired mPEG-SS-PzLL copolymer (Fig. S2 in ESI<sup>†</sup>). Successful synthesis of mPEG-SS-PzLL was also demonstrated by <sup>1</sup>H NMR analysis, in which the resonance peak from the mPEG moiety ( $\delta = 3.52$  ppm) and the PzLL fragment ( $\delta = 1.32$ – $1.77$ ,  $2.96$ ,  $4.99$  and  $7.34$  ppm) were observed (Fig. S3 in ESI<sup>†</sup>). The number of zLL residues in the copolymer chain was estimated by integrating signals from all methylene ( $\delta = 3.52$  ppm) and phenyl protons ( $\delta = 7.34$  ppm). This identified three distinct copolymer compositions containing on average 9, 15, or 30 zLL residues (*i.e.*, mPEG-SS-PzLL<sub>9</sub>, mPEG-SS-PzLL<sub>15</sub>, mPEG-SS-PzLL<sub>30</sub>, respectively, Table S1 in ESI<sup>†</sup>).

The critical micelle concentrations (CMCs) were estimated using pyrene as the fluorescence probe (Fig. S4 in ESI<sup>†</sup>), in which mPEG-SS-PzLL<sub>15</sub> exhibited the lowest CMC of 28 mg L<sup>-1</sup>. Further evidence for micelle formation was obtained by <sup>1</sup>H NMR spectroscopy. In contrast to the spectrum obtained in DMSO-*d*<sub>6</sub> (Fig. S3 in ESI<sup>†</sup>), signals from PzLL protons disappeared in D<sub>2</sub>O (Fig. S5 in ESI<sup>†</sup>), suggesting formation of compact association complexes where hydrophobic PzLL moieties are shielded by a hydrophilic PEG layer. DLS measurements showed the micelles had an average size of 302 nm in diameter (Fig. S6 in ESI<sup>†</sup>). TEM confirmed the distinct outline of polymer aggregates but at a smaller size in diameter (inset Fig. S6 in ESI<sup>†</sup>). As size determination by DLS is performed using aqueous suspension, it is conceivable that removal of water during TEM sample preparation may have contributed to shrinkage of micellar aggregates.

Nevertheless, both methodologies support the formation of polymer aggregates as micellar assemblies.

To investigate GSH-induced disassembly of mPEG-SS-PzLL nanomicelles, their aggregate size upon exposure to 10 mM GSH in PBS was monitored through 24 h by DLS (Fig. 2A). In the presence of 10 mM GSH, the mean diameter of the micelle significantly increased after 2 h from about 300 nm to about 419 nm, with concomitant broadening of the size distribution as demonstrated by the increase in PDI from 0.048 to 0.22. Formation of larger aggregates (> 1000 nm) was even more pronounced after 4 h. In contrast, the average micelle size remained constant for 24 h in the absence of GSH. Previously, Zhong and co-workers reported a similar increase in the size of redox-sensitive dextran-SS-poly( $\epsilon$ -caprolactone) copolymer aggregates in the presence of 10 mM DTT.<sup>11</sup> The authors concluded that reductive cleavage of the disulfide-coupled PEG shell thermodynamically forces hydrophobic fragments to rearrange into larger aggregates. This stimulus-induced rearrangement of micelles is predicted to facilitate the release of the encapsulated payload in the presence of reducing agents. Consequently, our results obtained with mPEG-SS-PzLL micelles, in the presence of 10 mM GSH, strongly suggest that micelle-encapsulated drugs will be rapidly released intracellularly in tumor cells.

We are interested in GSH-mediated drug release from redox-sensitive nanomicelles. The cytotoxic anticancer agent DOX was loaded into mPEG-SS-PzLL micelles by dialysis with 16.7% (w/w) loading efficiency. Fig. 2B summarizes the *in vitro* release of DOX from micelles in the presence and absence of GSH. At 2  $\mu$ M GSH, which physiologically corresponds to extracellular GSH concentrations (*e.g.*, plasma), less than 12% of the anticancer agent was released throughout a period of 36 h. Kinetically, the release rate under those conditions was comparable to that from control experiments performed in the absence of this biological reducing agent, suggesting that nonspecific leakage from intact micellar aggregates rather than redox-triggered disassembly of micelles as dominant drug release mechanism. Most importantly, however, DOX release was greatly accelerated at GSH concentrations comparable to intracellular levels reported for this biological antioxidant in tumor cells.<sup>15</sup> Since the therapeutic success of the proposed nanocarrier design critically depends on the timely removal of the PEG shell, data from this *in vitro* stability study predicted that GSH-triggered drug release will increase antitumor efficacy by almost 4-fold as compared to nonspecific drug leakage.

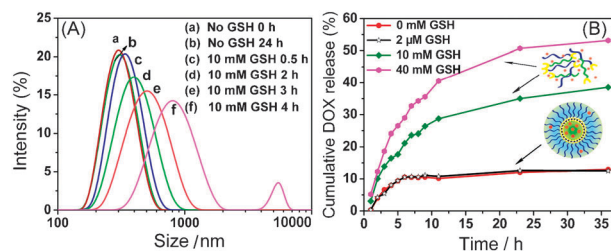


**Fig. 2** (A) Time-dependent changes in mPEG-SS-PzLL<sub>15</sub> micelle size in diameter upon exposure to 10 mM GSH as determined by DLS; (B) GSH-mediated drug release from DOX-loaded mPEG-SS-PzLL nanomicelles in PBS.

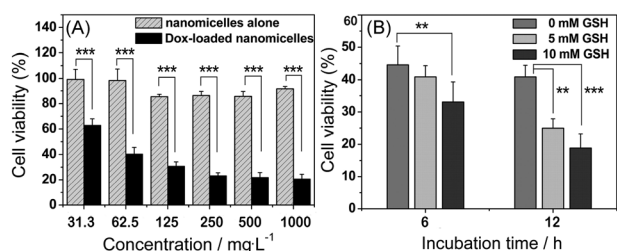


**Fig. 3** (A) Cell proliferation of MCF-7 breast cancer cells after 24 h incubation with mPEG-SS-PzLL<sub>15</sub> nanomicelles alone and DOX-loaded mPEG-SS-PzLL<sub>15</sub> nanomicelles. Data are presented as mean  $\pm$  SD ( $n = 6$ ); (B) Cell proliferation of MCF-7 cells after 6 h and 12 h incubation with DOX-loaded mPEG-SS-PzLL<sub>15</sub> nanomicelles (0.5 mg mL<sup>-1</sup>) in the presence of 0–10 mM extracellular GSH.

The therapeutic efficacy of DOX-loaded mPEG-SS-PzLL<sub>15</sub> nanomicelles was estimated *in vitro* by quantifying cell viability of human MCF-7 breast cancer cells using the MTT assay. As an important control experiment, it was demonstrated that micellar aggregates of mPEG-SS-PzLL copolymer without DOX do not significantly affect proliferation of this cell line up to a concentration of 1 mg mL<sup>-1</sup>. Inclusion of DOX into these nanomicelles effectively reduced cell viability of MCF-7 cells in a dose-dependent fashion (Fig. 3A).

It has been reported that extracellular shedding of PEG layers at the pathological target site tends to enhance drug release and facilitates uptake of the free drug by target cells.<sup>6</sup> To investigate whether DOX release triggered by different extracellular GSH concentrations similarly affects tumor cell viability, MCF-7 cells were incubated for 6 h and 12 h with DOX-loaded mPEG-SS-PzLL<sub>15</sub> nanomicelles using cell culture media supplemented with 0–10 mM GSH (Fig. 3B). Interestingly, addition of GSH to the cell culture media potentiated the inhibitory effect of DOX-loaded nanomicelles, especially after 12 h.

Confocal laser scanning microscopy (CLSM) of MCF-7 cells treated with DOX-loaded FITC-labeled nanomicelles further supported the hypothesis that increased extracellular GSH levels accelerate intracellular DOX accumulation (Fig. 4). The mean DOX fluorescence intensity of cells treated with 10 mM GSH increased by 1.68-fold as compared to the cells not treated with GSH (Fig. S7 in ESI<sup>†</sup>). Consistent with GSH-dependent rearrangement of micellar aggregates that resulted in accelerated and more quantitative release of

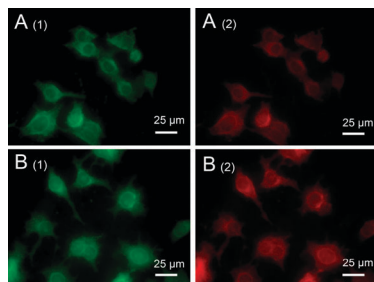


**Fig. 4** Representative CLSM micrographs of MCF-7 breast cancer cells incubated with DOX-loaded FITC-labeled nanomicelles for 4 h in the presence of (A) 0 mM extracellular GSH, (B) 10 mM extracellular GSH (green channel shows the fluorescence of FITC-labeled nanomicelles, whereas the red channel visualizes DOX fluorescence.)

DOX, it is conceivable that GSH-stimulated PEG enhanced antiproliferating efficacy after passive diffusion into MCF-7 cells. Alternatively, increased extracellular GSH levels may have augmented intracellular GSH levels, thus altering the release kinetics of DOX from internalized nanomicelles.

In conclusion, a novel, disulfide-linked block copolymer mPEG-SS-PzLL was successfully synthesized with the objective to prepare redox-sensitive nanocarriers for tumor-selective drug delivery. Upon exposure to tumor-relevant GSH levels, reductive cleavage of the disulfide-linked PEG shell initiates micellar rearrangement associated with the rapid release of the encapsulated payload. Cell proliferation assays performed with MCF-7 cells demonstrated the pharmacological efficacy of DOX released from mPEG-SS-PzLL<sub>15</sub> micelles in the presence of elevated GSH. Consequently, redox-sensitive mPEG-SS-PzLL nanocarriers are predicted to preferentially deliver encapsulated antitumor agents to desired tumor targets, which generally exhibit intracellular GSH concentrations 4-fold higher than normal cells. This will increase therapeutic efficacy and simultaneously decrease adverse events.

## Notes and references

- (a) R. Langer, *Nature*, 1998, **392**, 5–10; (b) K. Riehemann, S. W. Schneider, T. A. Luger, B. Godin, M. Ferrari and H. Fuchs, *Angew. Chem., Int. Ed.*, 2009, **48**, 872–897; (c) K. Knop, R. Hoogenboom, D. Fischer and U. S. Schubert, *Angew. Chem., Int. Ed.*, 2010, **49**, 6288–6308; (d) H. Otsuka, Y. Nagasaki and K. Kataoka, *Adv. Drug Delivery Rev.*, 2003, **55**, 403–419.
- (a) Y. Q. Shen, E. Jin, B. Zhang, C. J. Murphy, M. Sui, J. Zhao, J. Q. Wang, J. B. Tang, M. H. Fan, E. V. Kirk and W. J. Murdoch, *J. Am. Chem. Soc.*, 2010, **132**, 4259–4265; (b) H. Maeda, J. Wu, T. Sawa, Y. Matsumura and K. Hori, *J. Controlled Release*, 2000, **65**, 271–284.
- (a) S. M. Nie, *Nanomedicine*, 2010, **5**, 523–528; (b) H. Hatakeyama, H. Akita, K. Kogure, M. Oishi, Y. Nagasaki, Y. Kihira, M. Ueno, H. Kobayashi, H. Kikuchi and H. Harashima, *Gene Ther.*, 2007, **14**, 68–77.
- T. Masuda, H. Akita, K. Niikura, T. Nishio, M. Ukawa, K. Enoto, R. Danev, K. Nagayama, K. Ijuro and H. Harashima, *Biomaterials*, 2009, **30**, 4806–4814.
- F. M. Muggia, *J. Clin. Oncol.*, 1998, **16**, 811–811.
- B. Romberg, W. E. Hennink and G. Storm, *Pharm. Res.*, 2008, **25**, 55–71.
- X. Guo and F. C. Szoka, *Bioconjugate Chem.*, 2001, **12**, 291–300.
- (a) M. Z. Zhang, A. Ishii, N. Nishiyama, S. Matsumoto, T. Ishii, Y. Yamasaki and K. Kataoka, *Adv. Mater.*, 2009, **21**, 3520–3525; (b) R. J. Amir, S. Zhong, D. J. Pochan and C. J. Hawker, *J. Am. Chem. Soc.*, 2009, **131**, 13949–13952; (c) A. N. Koo, H. J. Lee, S. E. Kim, J. H. Chang, C. Park, C. Kim, J. H. Park and S. C. Lee, *Chem. Commun.*, 2008, 6570–6572.
- F. H. Meng, W. E. Hennink and Z. Zhong, *Biomaterials*, 2009, **30**, 2180–2198.
- S. Takae, K. Miyata, M. Oba, T. Ishii, N. Nishiyama, K. Itaka, Y. Yamasaki, H. Koyama and K. Kataoka, *J. Am. Chem. Soc.*, 2008, **130**, 6001–6009.
- H. L. Sun, B. N. Guo, X. Q. Li, R. Cheng, F. H. Meng, H. Y. Liu and Z. Y. Zhong, *Biomacromolecules*, 2010, **11**, 848–854.
- W. Gao, R. Langer and O. C. Farokhzad, *Angew. Chem., Int. Ed.*, 2010, **49**, 6567–657.
- W. W. Cleland, *Biochemistry*, 1964, **3**, 480–482.
- N. Ballatori, S. M. Krance, S. Notenboom, S. Shi S, K. Tieu and C. L. Hammond, *Biol. Chem.*, 2009, **390**, 191–214.
- (a) J. M. Estrela, A. Ortega and E. Obrador, *Crit. Rev. Clin. Lab. Sci.*, 2006, **43**, 143–181; (b) R. Franco, O. J. Schoneveld, A. Pappa and M. I. Panayiotidis, *Arch. Physiol. Biochem.*, 2007, **113**, 234–258; (c) R. Franco and J. A. Cidlowski, *Cell Death Differ.*, 2009, **16**, 1303–1314.